Article

The oncolytic adenovirus Ad-TD-nsIL12 in primary or progressive pediatric IDH wild-type diffuse intrinsic pontine glioma results of two phase I clinical trials

Xiao Qian[1,5], Weihai Ning[1,5], Jingjing Yang[1], Louisa Chard Dunmall [2], Hardev S. Pandha[3], Guanjie Shang[1], Yuduo Guo[1], Dongxu Zhang[1], Yanming Qu[1], Haoran Wang[1], Chunyu Gu[1], Mingshan Zhang[1], Yaohe Wang [2,6], Shengdian Wang [4,6] & Hongwei Zhang [1,6] ✉

Two single-center Phase I trials evaluated safety (primary endpoint) and preliminary efficacy (secondary endpoint) of oncolytic adenovirus Ad-TD-nsIL12 in primary (Group A, NCT05717712) and progressive (Group B, NCT05717699) pediatric patients with IDH wild-type (WT) diffuse intrinsic pontine glioma (DIPG). Studies employed single-arm and 3 + 3 dose-escalation design. 9 patients were enrolled in Group A and 6 in Group B. Group A completed the dose escalation, and no severe adverse events were observed. Enrollment in Group B was halted after Group A completed escalation. All patients experienced drug-related adverse events. In Group A, three partial responses and five stable diseases were documented, with a median overall survival (mOS) of 10.3 months after the first virus and 11.3 months after onset. In Group B, three patients had stable diseases, and three had progressive disease, with an mOS of 6.4 months after the first virus and 12.7 months after onset. Both groups demonstrated improved mOS from onset compared to the DIPG patients in our center's retrospective study (mOS, 8.3 months). Both groups showed increased lymphocytes post-treatment, but only Group A decreased after radiotherapy. These trials confirmed the safety of Ad-TD-nsIL12 and provided preliminary efficacy evidence, offering insights for future clinical applications in DIPG.

Diffuse intrinsic pontine glioma (DIPG) accounts for 80% of brainstem tumors in children[1]. Due to its deep location and high invasion, treatment options for this disease are extremely limited. While standardized radiotherapy has short-term benefits for DIPG, the prognosis remains poor, with little improvement over the past two decades. Patients typically experience progressive neurological decline, with a median overall survival (mOS) of less than one year (8–11 months) and a 5-year survival rate of less than 1%[2,3].

Historically, DIPG has been considered inoperable due to the high risks associated with surgery. However, the lack of surgical intervention has also impeded basic research on DIPG, limiting our understanding of the tumor immune microenvironment (TME) in situ. The

[1]Department of Neurosurgery, Sanbo Brain Hospital, Capital Medical University, Beijing, China. [2]Centre for Cancer Biomarkers & Biotherapeutics, Barts Cancer Institute, Queen Mary University of London, London, UK. [3]Department of Clinical and Experimental Medicine, University of Surrey, Guildford, UK. [4]National Laboratory of Biomacromolecules, Institute of Biophysics, Chinese Academy of Sciences, Beijing, China. [5]These authors contributed equally: Xiao Qian, Weihai Ning. [7]These authors jointly supervised this work: Yaohe Wang, Shengdian Wang, Hongwei Zhang. ✉e-mail: zhanghongwei@ccmu.edu.cn

advancements in stereotactic biopsy techniques have made tumor sampling more feasible, facilitating deeper insights into the genetic and immune characteristics of this disease[4]. For example, the histone modification at H3K27 has been identified as a hallmark of DIPG. Therefore, the World Health Organization (WHO) classified it as "diffuse midline glioma, H3K27-altered (DMG)" in the 5th edition of the Central Nervous System (CNS) tumor classification[5]. In addition, compared to pediatric hemisphere high-grade glioma (HGG), DIPG exhibits lower levels of CD8 + T cells and CD68+ macrophages, suggesting a relatively "cold" immune microenvironment with limited T cell infiltration, CD163+ macrophage presence, and cytokine expression[6]. These findings have spurred interest in exploring immunotherapy as a potential treatment strategy for DIPG.

The oncolytic adenovirus (OAd) has emerged as a promising treatment for cancer. It can remodel the suppressive tumor microenvironment to elicit robust anti-tumor immune responses and has been shown to synergize with other immunotherapies[7]. Several recent clinical trials have reported the safety and efficacy of oncolytic virus (OV) therapy in treating pediatric HGGs. In phase Ib clinical trial report on rhinovirus immunotherapy for recurrent pediatric HGGs, the median survival time appeared suboptimal, with only 4.1 months post-treatment[8]. Among the reported long-term survivors (beyond 22 months) was a patient with grade 3 glioma and IDH1 mutation (MUT)−a genetic marker associated with a relatively favorable prognosis[9]. Similarly, although DNX-2401 showed promising outcomes in primary DIPG patients, with a median survival of 17.8 months, one of the longer-term survivors also had H3 wild-type (WT) and IDH1 MUT[10].

The OAd used in this trial, Ad-TD, represents a new-generation, tumor-targeted replicating adenovirus modified with three gene deletions (E1A CR2, E1B19K, and E3gp19K) while retaining an intact E3B region, specifically designed to address the limited efficacy of earlier adenoviruses[11]. Beyond its oncolytic and immune-stimulatory properties, the virus is engineered with non-secreting IL-12 (nsIL12) to further enhance anti-tumor activity[12]. Preclinical studies have demonstrated the strong anti-tumor efficacy of Ad-TD-nsIL12 across multiple models without the typical safety concerns associated with unmodified IL-12[11–13]. We also validated the safety and efficacy of this virus in adult patients with recurrent HGGs[14]. Here, we present two phase I clinical trials evaluating the safety and feasibility of multiple intratumoral injections of Ad-TD-nsIL12 in pediatric DIPG patients with IDH WT, alongside preliminary evidence of its efficacy.

Results
Patient characteristics
Between January 2023 and September 2023, 18 patients were screened for the study. Detailed eligibility criteria have been listed in Tables S1 and S2. Three patients were excluded for not meeting the inclusion criteria, leaving a total of 15 patients who were enrolled in the study, nine in Group A and six in Group B. The enrollment and allocation process is illustrated in Fig. 1. Baseline characteristics of the enrolled patients are summarized in Table 1. The median age was 6 years in Group A and 6.5 years in Group B. The majority of the patients were male (73.3%). At baseline, the Lansky performance-status score (LPS) score was higher in Group A compared to Group B, with a median of 60 versus 55, respectively. Axial MRI scans (T2-based) revealed that both the largest tumor area and maximum measurable diameter were larger in Group A than in Group B. The median time from onset (defined as the first appearance of clinical symptoms) to the first virus treatment was 1.3 months in Group A. In contrast, Group B experienced significantly longer delay between onset and receiving virus treatment, with a range of 3.3 to 12.1 months. All patients were diagnosed with
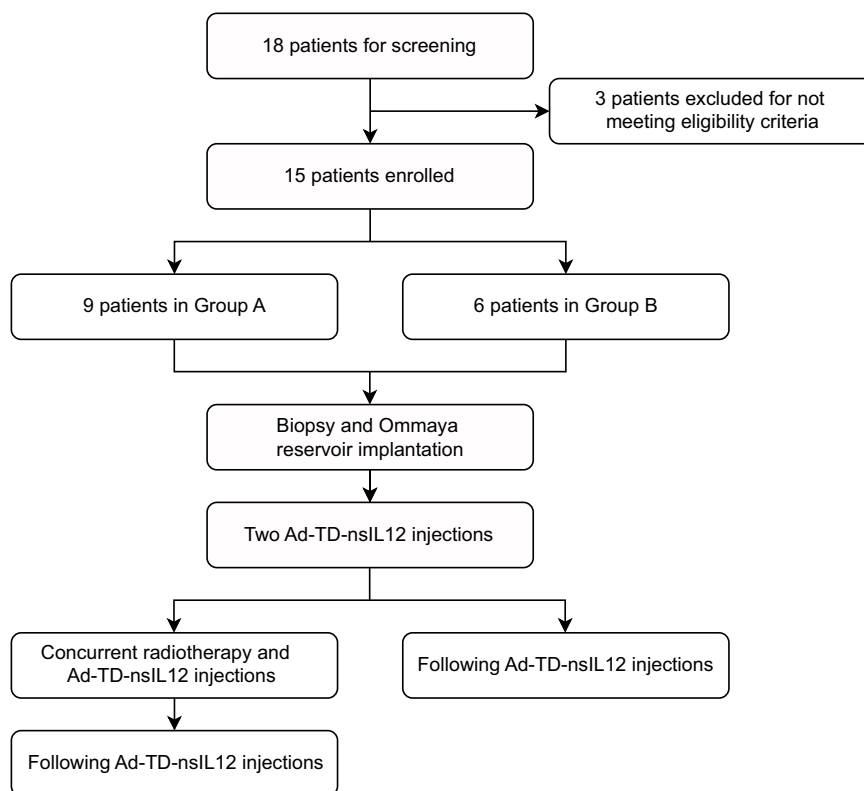

Fig. 1 | Patient screening and treatment process. A total of 18 patients were recruited. After screening, three patients were excluded for not meeting the eligibility criteria. Ultimately, 15 patients were enrolled and divided into 2 groups: nine in Group A and six in Group B. All patients underwent a biopsy and the implantation of an Ommaya reservoir, followed by two consecutive virus injections. Subsequently, patients in Group A received radiotherapy 2–6 weeks after the first virus treatment and following virus treatment, while patients in Group B received following virus treatment.

Table 1 | Baseline characteristics of patients

	Group A	Group B
N	9	6
Age (y)	6 (5–12)	6.5 (6–12)
Gender		
Female	3 (33.3%)	1 (16.7%)
Male	6 (66.7%)	5 (83.3%)
LPS score	60 (50–70)	55 (50–100)
Tumor size at baseline		
Largest area[a] (cm^2)	17.4 (9.6–25.5)	10.2 (5.8–12.4)
Longest diameter[b] (cm)	4.5 (3.3–5.1)	3.9 (2.5–4.3)
Duration between onset and first virus (mon)	1.3 (0.5–4.7)	6.7 (3.3–12.1)
Virus injection		
1	0	1
3	2	1
4	4	1
5	3	3
Treatment		
Radiotherapy[c] (Gy)	52.8 (52.2–55.8)	54 (50.4–54.0)
Glucocorticoid[d]	9 (100%)	5 (83.3%)
Anti-VEGF-A	3 (33.3%)	2 (33.3%)
Gene expression		
IDH1R132H WT	0 (0%)	0 (0%)
H3K27M MUT	9 (100%)	6 (100%)
GFAP	9 (100%)	6 (100%)
p53 MUT	8 (88.89%)	5 (83.3%)
ATRX	9 (100%)	6 (100%)
PDGFRa	9 (100%)	4 (66.7%)
EGFR	6 (66.7%)	4 (66.7%)

Categorical variables are presented using the *n* (n%), and descriptive variables are represented by the median (minimum value - maximum value).
LPS Lansky performance-status, *cm* centimeter, *VEGF-A* Vascular Endothelial Growth Factor A, *MUT* mutation, *WT* wild-type.
[a] Largest area on the axial view (T2 images).
[b] Largest diameter on the axial view (T2 images).
[c] For Group A, radiotherapy refers to the standard treatment post-virus. For Group B, radiotherapy refers to the initial treatment pre-virus.
[d] Glucocorticoid use during radiotherapy is excluded.

DIPG through histology and imaging. Every patient had H3K27M MUT, while none had IDH MUT. Additionally, p53 MUT were presented in 88.89% of Group A and 83.3% of Group B. The detailed genetic profiles of the tumors are provided in Table S3.

Treatment procedure

Before receiving viral therapy, all patients underwent stereotactic biopsy and Ommaya reservoir implantation for continuous viral administration, with the reservoir tip positioned at the center of the tumor lesion confirmed by post-treatment CT and MRI (Fig. S1a). Post-treatment FLAIR imaging allowed us to visualize the biopsy site and the areas of virus infiltration (Fig. S1b). In this study, we administered OV injections at different time points, specifically before radiation therapy (Group A) and progression after radiation therapy (Group B). All patients in Group A received multiple virus treatments (Fig. 2a). Early dual-virus treatment with an interval of 3 days was administrated to stimulate immunity. All patients in Group A then received radiation therapy after these first two virus injections. Follow-up virus injections were performed approximately every 3 weeks. Except for two patients in Group A who couldn't come to the hospital during radiotherapy due to personal reasons, the rest of the patients had one viral treatment during the radiotherapy course. The fourth and fifth viral treatments (if administered) were conducted post-radiotherapy. Group B patients were treated using the same virus injection regimen but did not undergo concurrent radiotherapy (Fig. 2b). In Group B, one patient's guardian (patient B01) refused further treatment for personal reasons after the first injection but completed subsequent follow-ups. Other patients in Group B received multiple injections.

The number of injection sites was also a critical factor in OV therapy. Depending on MRI findings, the number of Ommaya reservoirs implanted varied. Six patients had two Ommaya reservoirs inserted, while the remaining patients had one (Table 2). Patient A01 underwent two separate Ommaya reservoir implantations. Initially, the tumor necrosis was located on the right side of the brainstem (Fig. 2c). However, after 8 weeks, necrosis was observed on the left side, confirmed to be tumor progression rather than pseudo-progression by biopsy. Immunohistochemical (IHC) stainings for adenovirus E1A and hexon proteins on tissues post-therapy were negative (Fig. S2), likely because the biopsy site was distant from the initial injection site. This outcome underscored the need for additional injection sites, leading to a second Ommaya reservoir implantation. At the 6-month and 12-month follow-ups, the patient showed a significant reduction in tumor volume.

Tumor progression and radiation therapy can both lead to peritumoral edema. During follow-up, 14 patients were treated with low-dose glucocorticoids when necessary to control symptom, and 5 patients received Bevacizumab (Table S4). No MRI evidence of pseudo-progression related to glucocorticoid use was observed. Two patients in Group B underwent a second radiation therapy following tumor progress.

Safety and pharmacokinetics

All patients underwent stereotactic biopsy guided by the REME robot and Ommaya reservoir insertion for subsequent virus injections. Two patients developed hematomas at the surgical site (verified by post-surgery CT), leading to breathing difficulties and a reduced cough reflex. These two patients required admission to intensive care unit but did not require respiratory support. Importantly, no neurological dysfunction related to the surgery was observed in both patients during follow-up.

In Group A, the virus dose was escalated to the maximum dose of 3×10^{10} vp and no grade 3 or higher treatment-related adverse events (AEs) were documented. Consequently, the evaluation of the maximum tolerated dose (MTD) was not reached. Due to a delay in the enrollment of Group B. enrollment was discontinued after the completion of the dose escalation and safety assessment in Group A. All enrolled patients experienced treatment-related AEs, all of which were grade 1 or 2 (Table 3). The dose-tiered AEs are detailed in Table S5. The most common virus-related AEs were fatigue (100%), vomiting (87%) and fever (87%). Fever typically occurred approximately 24 h after OV injection, generally requiring only symptomatic treatment, such as physical cooling or oral antipyretics, and subsided within 48 hours. During this period, other symptoms like fatigue, vomiting, and dizziness were also observed. Importantly, seizures were recorded during the patient's (A08) follow-up period but did not occur during the periviral treatment period (Table S5). They were reported by the patient's family at their local residence and occurred only once, at a time when the patient had already developed ventricular dissemination of the tumor.

In this study, we assessed the pharmacokinetics of the drug by quantifying viral DNA in both serum and cerebrospinal fluid (CSF) using qPCR. Adenovirus DNA was detected in the peripheral serum of patients A02 and A03 (Table S6). No typical signs of ventriculitis or meningitis were observed in our patients post-injection. Additionally, no viral DNA was detected in the CSF samples obtained from the patients (patient A01, A02, B03, and B04). IL12 protein was detected in the serum of patient A04, A09, B03, B04, and B05, but not in the CSF.
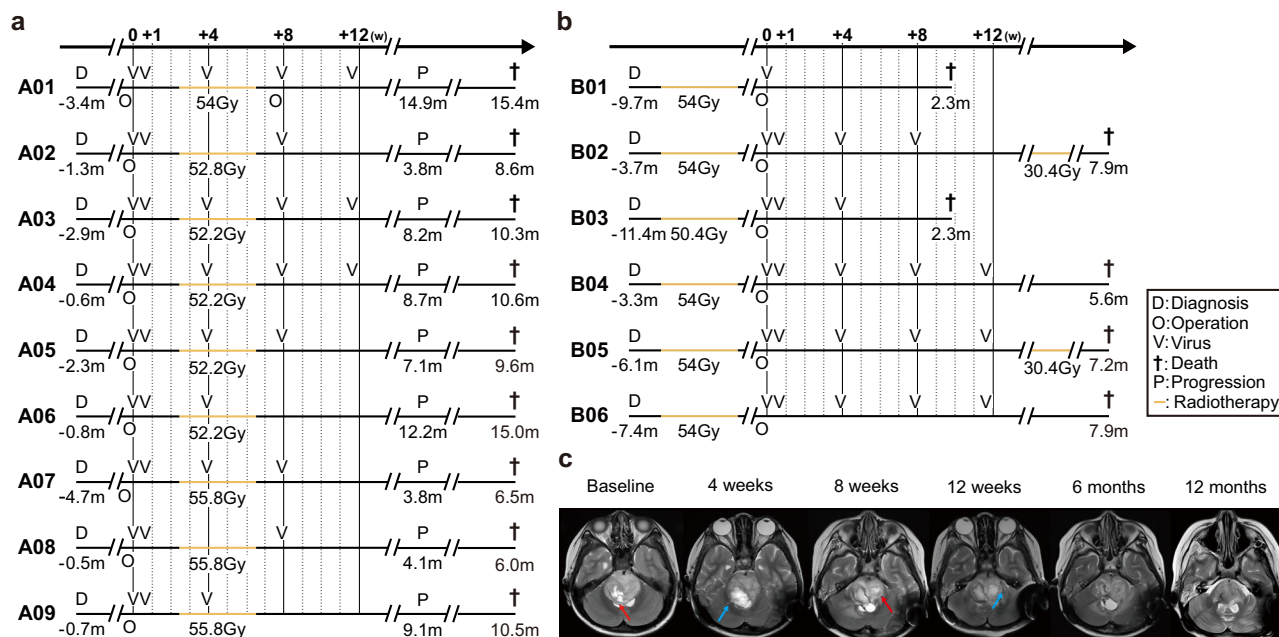
Fig. 2 | Treatment process and tumor response for patients in Group A and Group B. a Treatment timeline for Group A patients. All patients started radiotherapy within 4 weeks after baseline, indicated by a yellow line, and received multiple virus treatments. Except for patients A02 and A08, other patients received a virus treatment during radiotherapy. **b** Treatment timeline for Group B patients. All patients underwent radiotherapy before baseline. Except for patient B01, all other patients received multiple viral injections. Patients B02 and B05 underwent a second round of radiotherapy. **c** Treatment process and tumor MRI scan changes for patient A01. The baseline scan showed the lesion with central necrosis of the tumor (red arrow) primarily on the right side of the brainstem. At 4 weeks, the Ommaya reservoir was observed (blue arrow). At 8 weeks, progression on the left side of the brainstem was noted, with significant central necrosis (red arrow). A biopsy confirmed the presence of the tumor over radiation necrosis, followed by a second reservoir implantation on the left side. The second Ommaya reservoir was identified at 12 weeks (blue arrow). Significant tumor shrinkage was observed at the 6-month follow-up, with improved regularity of the fourth ventricle. By the 12-month follow-up, the brainstem morphology had nearly normalized.

However, no adenovirus DNA was detected concurrently in IL-12 positive serum samples. Therefore, the detection of IL-12 in peripheral blood cannot be simply attributed to viral shedding. Additionally, patients with adenovirus DNA and IL-12 detected in serum did not exhibit virus-related AEs at the time of sample collection.

Host immune response to the Ad-TD-nsIL12

To investigate the systemic immune responses to Ad-TD-nsIL12, the cell composition in the peripheral blood of patients were monitored by flow cytometry during follow-up (Fig. S3). In Group A, the leukocytes of patients peaked in the 1st week after the initial two consecutive treatments, exceeding the baseline and subsequent follow-up levels (Fig. 3a). The leukocyte (CD45 +) levels at baseline and subsequent follow-ups were relatively similar. One week after treatment, the counts of CD3 +, CD4 +, and CD8 + T cells increased compared to baseline but subsequently decreased. At 8 and 12 weeks, the T cell levels were even lower than baseline. This decrease was significant for CD3+ and CD4+ cells at 8 and 12 weeks, while CD8+ cells showed significance at 8 weeks (compared to 1-week level).

In Group B, two patients who did not survive to 12 weeks were excluded from the statistical analysis due to the lack of corresponding samples (Fig. 3b). The results of the blood cell components for all patients are recorded in Fig. S4. In Group B, peripheral blood leukocytes significantly increased at 4 and 8 weeks compared to baseline. The changes in CD3 +, CD4 +, and CD8 + T cells differed from those in Group A. One week after the two consecutive OV treatments, these peripheral T cell counts increased and remained higher than baseline in subsequent follow-ups.

The above results indicate that although the lymphocyte counts in the peripheral blood increased in both groups after the two consecutive OV injections, the subsequent changes differed. The continuous decline in lymphocyte counts post-radiotherapy in Group A

may be related to the radiotherapy, which began between 1 and 4 weeks and ended between 4 and 8 weeks. Despite some patients receiving additional OV treatment during radiotherapy, this decline was not reversed. Interestingly, this decline was not observed in Group B patients in whom worse survival outcomes were recorded.

Repeated measures ANOVA showed no significant differences in leukocytes, CD3 +, CD4 +, and CD8+ cell counts between Group A and Group B (Fig. S5a), suggesting no significant differences in leukocyte and lymphocyte counts within 3 months post-treatment. However, at baseline, the cell counts in Group A were significantly higher than those in Group B, which may be related to the poorer nutritional status and immune suppression of Group B patients in the later stages of the disease[15]. This difference might also contribute to the varied prognoses between the two groups. The cytokine levels in Group A showed no significant differences with time after treatment, while in Group B, IFN-γ, TNF-α, and IL-6 levels were increased after the first two treatments, with a significant increase observed in IL-6 (Fig. S5b).

The alteration of neutralizing antibody against Adenovirus

In Group A, 6 patients were negative for adenovirus neutralizing antibodies in the serum before treatment, and 3 were positive (Fig. S6). In Group B (with a total of 5 patients tested), 4 patients were negative for adenovirus neutralizing antibodies at baseline. The serum neutralizing antibody titers were increased after treatment in both groups. Of note, among the three positive patients in Group A before the virus treatment, two achieved partial response (PR).

Efficacy

In Group A, tumor shrinkage was observed in five patients, while the remaining four experienced varying degrees of tumor enlargement compared to baseline (Fig. S7a). Among the five patients with tumor

Table 2 | Detailed clinical information of patients

No.	Age	Gender	Assigned Dose (vp)	LPS at Admission	Largest Area (cm²)	Longest Diameter (cm)	Time Between First Virus and RT (day)	RT (Gy)	Number of Ommaya Reservoir	Virus Injections	Best Response	OS(After first virus, mon)	OS (After onset, mon)
A01	6	female	3×10^9	50	23.0	4.8	21	54	2	5	PR	15.4	18.7
A02	6	female	3×10^9	60	21.7	3.8	21	52.8	2	4	SD	8.6	9.9
A03	10	male	3×10^9	50	25.5	5.1	14	52.2	2	5	PR	10.3	13.1
A04	5	male	1×10^{10}	70	20.0	5.0	20	52.2	1	5	SD	10.6	11.2
A05	7	male	1×10^{10}	50	10.9	4.2	21	52.2	2	4	PR	9.6	11.9
A06	6	male	1×10^{10}	70	17.4	4.7	25	52.2	1	3	SD	15.0	15.8
A07	10	male	3×10^{10}	70	16.2	4.5	20	55.8	1	4	PD	6.5	11.2
A08	12	male	3×10^{10}	60	9.6	3.3	31	55.8	1	4	SD	6.0	6.5
A09	6	female	3×10^{10}	70	16.3	4.4	21	55.8	1	3	SD	10.5	11.3
B01	6	male	3×10^9	50	7.9	3.3	-	54	1	1	PD	2.3	12.1
B02	6	male	3×10^9	90	5.8	2.5	-	54	1	4	SD	7.9	11.6
B03	7	male	3×10^9	50	10.3	4.3	-	50.4	1	3	SD	2.3	13.7
B04	6	male	1×10^{10}	50	12.4	4.0	-	54	2	5	PD	5.6	9.0
B05	12	Female	1×10^{10}	100	10.0	3.7	-	54	1	5	SD	7.2	13.2
B06	8	male	1×10^{10}	60	12.0	4.0	-	54	2	5	PD	7.9	15.2

vp virus particle, *LPS* Lansky performance-status, *RT* radiotherapy, *PR* partial response, *SD* stable disease, *PD* progressive disease, *OS* overall survival.

shrinkage, four showed a reduction of more than 25%, while one had a reduction of less than 25%. Of the four patients with a reduction greater than 25%, one experienced a shrinkage for less than 8 weeks. Among the four patients with tumor enlargement, one exhibited an increase of more than 25%. Consequently, in Group A, three patients were classified as having a PR, five as stable disease (SD), and one as progressive disease (PD). The objective response rate (ORR) was 33.3%, and the disease control rate (DCR) was 88.9%. The mOS in Group A following viral therapy was 10.3 months after the first virus (range: 6–14.4 months) and 11.3 months after onset (range: 6.5–18.7 months). Two patients survived for more than 12 months, resulting in a 12-month survival rate of 22.2%. Stratifying survival by treatment dose reveals that patients with PR and longer survival durations were found in the medium and low dose groups rather than in the high dose group.

Compared to Group A, Group B exhibited poorer tumor response and survival outcomes from first virus injection (Fig. 4a), with no recorded response or disease control. However, when measured from disease onset, there was no significant difference between the two groups (Fig. 4b). All six enrolled patients in Group B experienced varying degrees of tumor enlargement compared to baseline (Fig. S7b). Among them, three patients had tumor enlargement exceeding 25%, classified them as PD, while the other three were classified as SD. Consequently, both the ORR and DCR in Group B were lower than those in Group A. The mOS in Group B following viral therapy was 6.4 months after the first virus (range: 2.3–7.9 months) and 12.7 months after onset (range: 9.0–15.2 months). For both tumor response and post-intervention mOS, Group B was worse than Group A. These results prompted consideration of the effectiveness of OV therapy following radiotherapy may be inferior to initiating treatment from the primary tumor.

To further validate the treatment efficacy, we conducted a retrospective study to compare the survival outcomes (from disease onset) of Group A and B patients with cases in our center. Detailed eligibility criteria have been listed in Table S7. From an initial cohort of 56 patients, 35 were excluded, yielding 21 analyzable cases (Fig. S8). The patients' clinical characteristics have been concluded in Table S8. The analysis revealed that both Group A and B demonstrated longer mOS compared to our institutional historical data with an mOS of 8.3 months (Fig. 4c, d). These findings collectively indicate that viral therapy resulted in clinically significant survival prolongation.

Tumor immune micro-environment alterations

IHC staining of tissue samples from patient A01 (the only patient for whom post-treatment biopsy samples were available) showed no significant changes in CD3+, CD4+, and CD8+ cell expression levels 2 months after initial treatment (Fig. 5). In contrast, the post-treatment sample showed a significant increase in CD68+ cells, indicating increased macrophage infiltration. Further staining revealed consistently low levels of CD86+ cells before and after treatment, while CD163+ cells slightly increased but not significantly (Fig. 5). Low levels of CD86+ suggest that macrophages are predominantly in an M2-like, alternatively activated state rather than an M1-like. The slight increase in CD163+ cells supports this, as M2 macrophages are known to promote tumor growth and angiogenesis. IL12 levels in the post-treatment sample remained unchanged compared to pre-treatment levels (Fig. S9).

Discussion

This report presents results from two phase I clinical trials investigating the safety of an OV, Ad-TD-nsIL12, for treating pediatric DIPG patients. The trial enrolled 15 patients divided into two groups based on medical history: nine in Group A and six in Group B. The preset virus levels were all safely administered repeatedly, and the study did not determine a MTD for multiple intratumoral injections of Ad-TD-nsIL12 in pediatric patients with DIPG. In addition, this study confirmed the safety of using an Ommaya reservoir in pediatric patients with DIPG, which enabled multiple bedside viral injections, eliminating the need for repeated surgical procedures during treatment and significantly improving the quality of life for patients throughout therapy. This trial also preliminarily validated the effectiveness of Ad-TD-nsIL12 in DIPG patients and explored the combination of this virus with radiation therapy.

OVs are being actively explored for various malignancies, including pediatric HGG. The G207 has demonstrated therapeutic efficacy in the treatment of pediatric supratentorial HGG, with a median survival of 12.2 months, and 4 patients surviving for more than 18 months post-treatment[16]. However, compared to supratentorial HGG, DIPG exhibits distinct biological and clinical characteristics, as it belongs to the unique subtype of DMG. Notably, other OVs such as DNX-2401 have also shown potential therapeutic effects in preclinical studies and clinical trials for DIPG[10,17,18]. Among the two patients with

Table 3 | Adverse events attribute to Ad-TD-nsIL12

	Grade 1	Grade 2	Grade 3	Grade 4	n (%)
Ear and labyrinth disorders					
Tinnitus	1	0	0	0	1 (7%)
Eye disorders					
Extraocular muscle paresis	1	0	0	0	1 (7%)
Gastrointestinal disorders					
Dyspepsia	1	0	0	0	1 (7%)
Vomiting	13	0	0	0	13 (87%)
General disorders and administration site conditions					
Fatigue	15	0	0	0	15 (100%)
Fever	9	4	0	0	13 (87%)
Injection site reaction	1	0	0	0	1 (7%)
Infections and infestations					
Upper respiratory infection	0	2	0	0	2 (13%)
Lymphocyte count decreased	2	0	0	0	2 (13%)
Musculoskeletal and connective tissue disorders					
Muscle weakness upper limb	1	0	0	0	1 (7%)
Nervous system disorders					
Depressed level of consciousness	7	0	0	0	7 (47%)
Dizziness	11	0	0	0	11 (73%)
Dysesthesia	1	0	0	0	1 (7%)
Headache	5	4	0	0	9 (60%)
Hypersomnia	7	0	0	0	7 (47%)
Memory impairment	1	0	0	0	1 (7%)
Spasticity	0	1	0	0	1 (7%)
Dyspnea	1	0	0	0	1 (7%)
Skin and subcutaneous tissue disorders					
Rash	0	1	0	0	1 (7%)

Adverse Events (AEs) are graded according to NCI-CTCAE 5.0.
The same AE in one patient is recorded once by the most severe case.

the longest survival following DNX-2401 treatment, one patient's tumor was characterized by H3 WT and IDH1 MUT. This study aimed to assess the safety of repeated use of Ad-TD-nsIL12 in IDH WT DIPG patients, focusing on dose safety and the feasibility of multiple intratumoral injections into the brainstem. For dose safety, based on preclinical studies and clinical trials in adults with recurrent HGG[14], three escalating dose levels were tested: 3×10^9vp, 1×10^{10}vp, and 3×10^{10}vp. Despite not reaching the MTD, results suggested that higher doses were unnecessary. Firstly, tumor response was not documented at higher doses; instead, better therapeutic effects were observed at lower concentrations. Additionally, in adult trials, a dose of 5×10^{10}vp resulted in SAEs. Therefore, dose escalation was terminated. All recorded grade 2 AEs related to treatment were manageable with symptomatic treatment, indicating that multiple intratumoral injections of Ad-TD-nsIL12 up to 3×10^{10}vp are safe in children with DIPG. The IL-12 can significantly enhance both innate and adaptive immune responses in the host, stimulate the secretion of IFN-γ, and remodel the tumor microenvironment[19]. However, systemic administration of IL-12 is associated with substantial toxicity, which limits its broad application in antitumor therapy. Previous studies have demonstrated an adenoviral vector (Ad-RTS-hIL-12) carrying controllably expressed IL-12 which is activated by veledimex (VDX)[20,21]. However, the phase I

study reported AEs at all dose levels, with a higher incidence at higher doses, which prevented the achievement of the predefined MTD. Additionally, cytokine release syndrome (CRS) was observed across various dose levels, accompanied by significant increases in serum and CSF levels of IFN-γ and IL-12 (observed in one patient). In this study, the nsIL-12 encoded by Ad-TD-nsIL-12 demonstrated a favorable safety profile, with no observed CRS or other severe adverse reactions.

For drug administration, compared to stereotactic puncture injections in the brain hemispheres, the brainstem poses greater risks. To mitigate this risk, we implanted an Ommaya reservoir for repeatable bedside injections. Although two patients developed small hematomas near the surgical site, they did not suffer lasting neurological deficits. Other patients also did not experience neurological deficits associated with biopsy surgery or the Ommaya reservoir implantation. Based on these results, the administration of OVs via an Ommaya reservoir proved to be a safe and feasible approach. This method eliminates the need for repeated stereotactic injections during treatment, thereby significantly enhancing the quality of life for patients throughout both the treatment and follow-up periods. However, using the Ommaya reservoir presents challenges. Firstly, while the Ommaya reservoir has multiple side ports for virus injection and infiltration, it is inadequate for addressing diffuse lesions such as DIPG, as evidenced by the absence of E1A and hexon proteins in post-treatment samples in one patient. Consequently, in some patients with larger tumors, we used two Ommaya reservoirs to expand the area of viral infection. Moreover, ensuring precise targeted delivery to the tumor center and preventing reflux of the injected liquid are challenges that may become more pronounced as the disease progresses.

Previous trials of OVs for DIPG, such as with DNX-2401, used a single injection before radiotherapy[10]. How to combine multiple OV injections with the mandatory radiotherapy requires further investigation. In this study, we administered first two consecutive injections 3 days apart, aiming to align with the T cell activation and proliferation timeline[22], with subsequent virus injections at 3-week intervals (±4 days). Peripheral blood lymphocyte counts increased after the initial two consecutive OV injections in both groups, indicating that this approach is feasible and successfully induces systematic immunity. However, subsequent changes differed between the groups. Lymphocyte counts in Group A continuously declined during follow-up after radiotherapy. At 8 and 12 weeks, lymphocyte counts were significantly lower than at 1 week and below baseline levels. In contrast, in Group B, lymphocyte counts remained higher than baseline levels during the 8- and 12-week follow-ups. This suggests that although radiotherapy is effective in the short term for DIPG patients, it may negatively impact patients' immune function and does not improve the long-term prognosis[23]. In the study of G207 application in pediatric patients with HGGs, long-term intratumoral T-cell recruitment was detected in post-treatment samples, although it was not verified whether these T cells were tumor-specific[16]. In this study, we analyzed post-treatment samples from patient A01. The IHC analysis showed increased infiltration of CD68+ macrophages, without an increase in CD4+ and CD8 + T cells, and no viral protein was detected. This can be attributed to several reasons: The sample was collected from a new progression area on the left side, which was far from the initial virus injection site. These results suggest that additional multi-point injections may be necessary, as the virus itself demonstrated limited spreading to the secondary biopsy site. Furthermore, the second biopsy was performed after radiotherapy, which is known to induce M2 polarization[24] and lymphocyte depletion[25]. Considering all these factors, the lack of lymphocyte infiltration and the presence of M2 polarization at the local site may be strongly associated with radiotherapy, local rapid progression, and insufficient virus spreading. Therefore, multiple injections in different directions might be required.

Although Group A and Group B do not constitute a strictly controlled comparison, we attempted to analyze the post-intervention OS
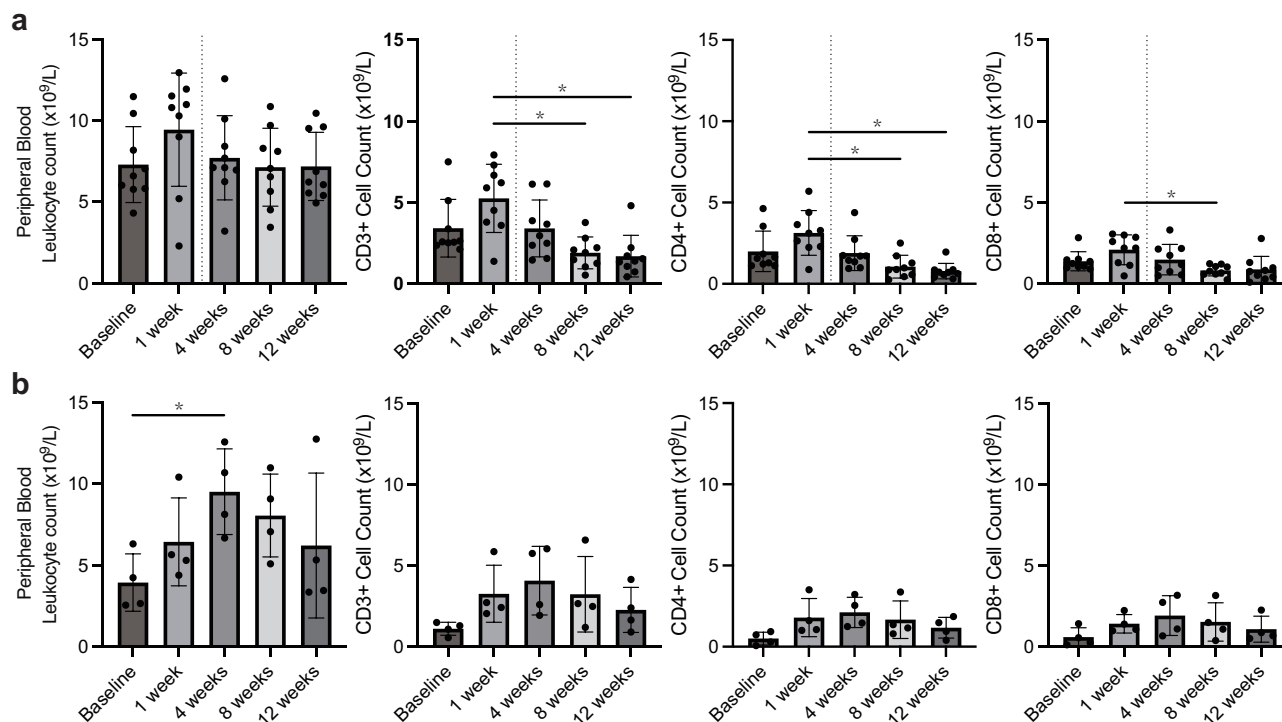
Fig. 3 | Changes over time in leukocytes, CD3+, CD4+, and CD8+ cell counts in the peripheral blood of patients. a In Group A ($n = 9$), CD45+ cell level in peripheral blood was higher 1 week than baseline and remained consistent at 4, 8, and 12 weeks. CD3+, CD4+, and CD8+ cell counts increased 1 week after baseline but then gradually decreased over time. Among these, CD3+ cells showed a significant decrease at 8 weeks ($p = 0.018$) and 12 weeks ($p = 0.002$) compared to 1 week, CD4+ cells exhibited a significant decrease at 8 weeks ($p = 0.012$) and 12 weeks ($p = 0.001$) compared to 1 week, and CD8+ cells also demonstrated a significant decrease at 8 weeks compared to 1 week ($p = 0.047$). **b** In Group B ($n = 4$), CD45+, CD3+, CD4+, and CD8+ cell levels gradually increased after baseline and remained above baseline levels within 12 weeks. Among these, compared to baseline, there was a significant increase in CD45+ cells at 4 weeks ($p = 0.007$). Repeated measures ANOVA Test, * indicates $p = 0.05$ and error bars represents mean ± standard deviation and test was two-sided. Source data are provided as a Source Data file.
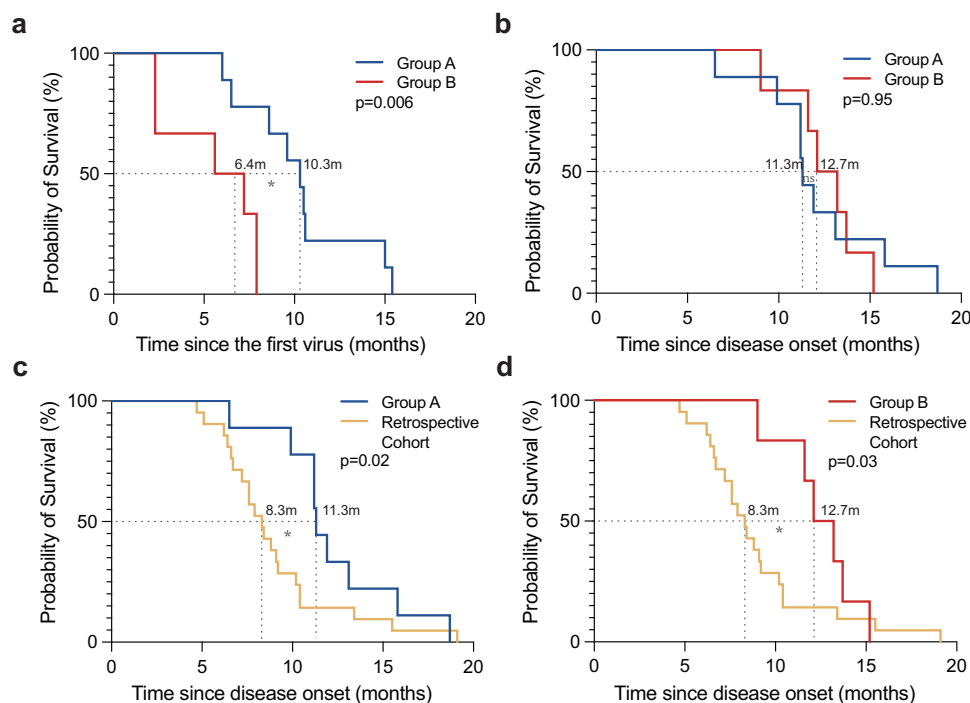
Fig. 4 | Comparison of survival outcomes between Group A, Group B and retrospective cohort patients. a Comparison of survival time between Group A ($n = 9$) and Group B ($n = 6$) patients after the first virus injection, with Group A demonstrating better median overall survival than Group B. **b** Comparison of survival time from the onset of the disease between Group A and Group B, showing no significant difference between the two groups. **c** Comparison of survival time between Group A and the retrospective cohort ($n = 21$) from the onset of the disease, showing better median overall survival in Group A than in the retrospective cohort. **d** Comparison of survival time between Group B and the retrospective cohort from the onset of the disease, demonstrating better median overall survival in Group A than in the retrospective cohort. Kaplan-Meier survival curve curve, * indicates $p = 0.05$.
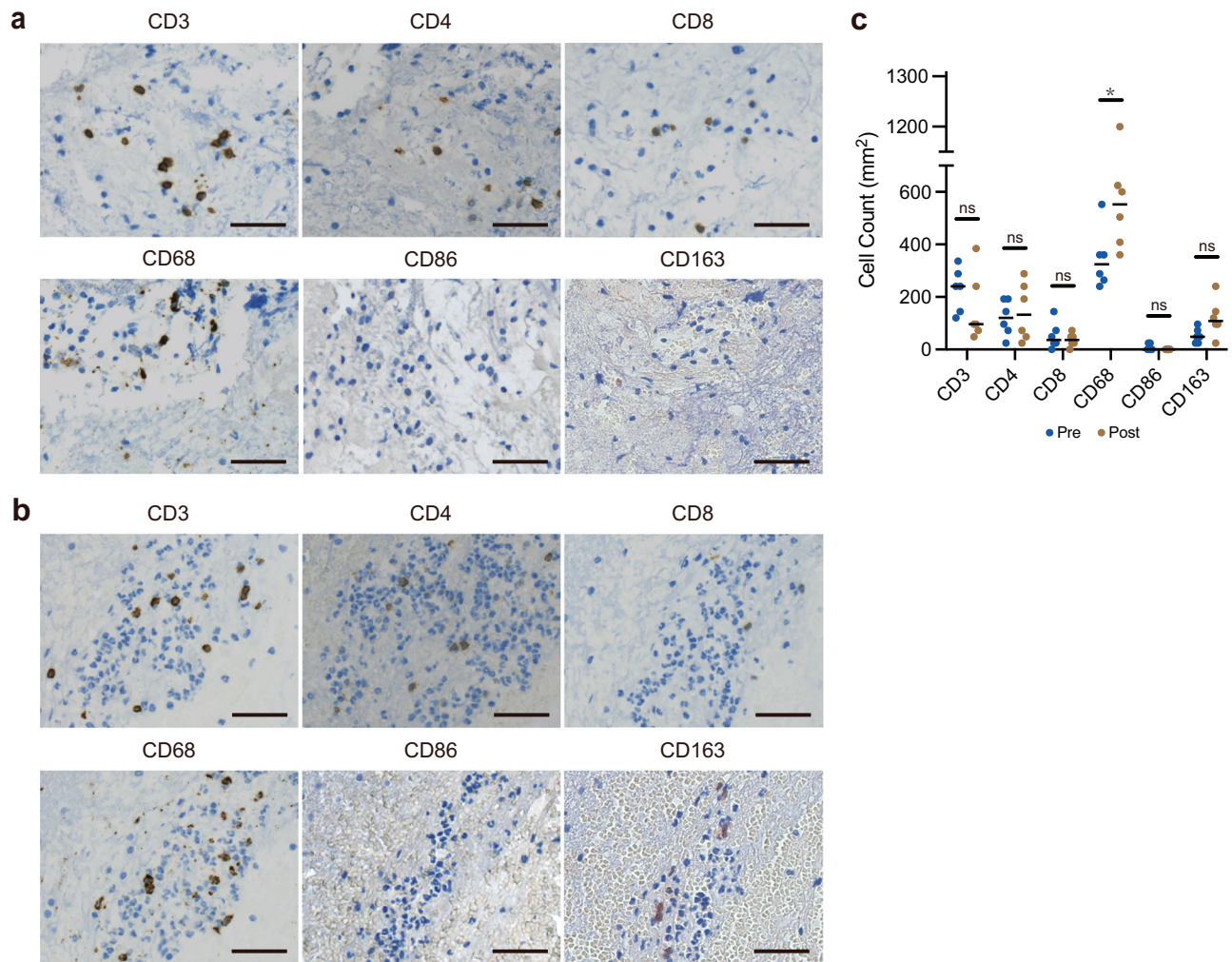
Fig. 5 | Changes in immune cells within tumor samples before and after viral therapy of patient A01. a Representative immunohistochemical images of immune cells in biopsy samples taken before viral therapy (scale bar 50 μm). **b** Representative immunohistochemical images of immune cells in biopsy samples taken after viral therapy (scale bar 50 μm). **c** Quantification of immunohisto-chemical results before and after treatment, showing no significant changes in CD3+, CD4+, and CD8+ cells pre- and post-treatment (*n* = 6). However, there is a significant increase in CD68+ cells in samples obtained after viral therapy (*p* = 0.03). Additionally, the proportion of CD86+ cells in the tissue remained very low before and after treatment, while the proportion of CD163+ cells increased after treatment but did not reach statistical significance. Wilcoxon signed-rank test, bars represent median and statistical test was two-sided, * indicates *p* = 0.05. Source data are provided as a Source Data file.

to explore the potential relationship between the timing of viral intervention and patient prognosis. The mOS in Group A was 10.3 months, significantly longer than 6.4 months in Group B. According to Response Assessment in Pediatric Neuro-Oncology (RAPNO) standards, the ORR in Group A was 33.3%, with a DCR of 88.9%, and two patients survived for more than 15 months. This dif-ference may be partially attributed to the different baseline immune status of the patients. Comparing cell counts between Group A and Group B reveals that baseline levels of leukocytes, CD3 + , CD4 + , and CD8 + T cells were higher in Group A, and the increase after OV treat-ment was less pronounced than in Group B, indicating that leukocyte and lymphocyte counts are lower in patients with recurrent tumors after radiotherapy, which could negatively affect the efficacy of immunotherapy. Considering the systemic immune changes in patients after treatment and the difference in lymphocyte counts between groups at baseline, early intervention with Ad-TD-nsIL12 appears to be a better choice, as the patient's immune function is more robust at this stage. The intervention of radiotherapy may significantly impact the already stimulated immune function. Therefore, the use of OVs chal-lenges the current treatment approach for DIPG, which relies on radiotherapy as the standard of care[26]. However, due to ethical restrictions and limitations in sample collection from pediatric patients, we were unable to perform further in-depth analysis of the diversity of the T-cell receptor (TCR) and its functional studies on patient blood samples. Another intriguing observation in our study is that the tumor response in Group A patients was primarily observed at medium and low dose levels, rather than at the highest dose level. This may be related to the fact that high doses of OVs may paradoxically suppress anti-tumor immune responses. According to a report by Liu et al., adenovirus therapy significantly increases the proportion of Tregs and M2-like macrophages in the tumor microenvironment, thereby attenuating antitumor effects[27]. Another research also demonstrated that OV therapy (M1) can upregulate PD-L1 expression in tumor cells, thereby weakening the antitumor activity of CD8 + T cells. Moreover, OVs may promote tumor immune evasion by upregulating PD-L1 or secreting immunosuppressive factors (e.g., IL-10, TGF-β)[28]. These findings provide important guidance for future studies regarding virus dose selection and the advancement of combination therapy strategies.

This study has several limitations. The small sample size may affect efficacy assessments. Although sequencing would provide more precise results, due to the insufficient left tumor materials, we were

unable to perform sequencing analysis. While we observed systemic immune responses through peripheral lymphocyte monitoring, these findings should be interpreted cautiously as they may not fully reflect TME changes. The availability of only one post-treatment tumor sample limits results about post-treatment TME assessment. Additionally, while clinically necessary, the use of low-dose corticosteroids for managing cerebral edema and neurological symptoms could represent a potential confounding factor in immune response analyses. These limitations highlight the need for future studies with larger cohorts, modified tissue sampling protocols, and more comprehensive immune monitoring strategies to better understand the treatment's effects on both systemic and tumor immunity.

This study evaluated for the first time the safety of the OV Ad-TD-nsIL12 in pediatric DIPG patients. Among the three planned doses, no SAEs occurred, and the MTD was not reached, demonstrating that repeated administration of Ad-TD-nsIL12 at doses up to 3×10^{10}vp is safe in DIPG patients. Additionally, this study explored the safety of using an Ommaya reservoir for the delivery of OVs in pediatric patients with DIPG. Furthermore, the study preliminarily assessed the effectiveness of Ad-TD-nsIL12 in DIPG patients, with three patients achieving PR in Group A, resulting in an ORR of 33.3%. This study innovatively utilized Ommaya reservoirs for OV injection, addressing the need for multiple injections and reducing the risk of brain tissue puncture injuries. Early intervention with OV therapy appears to be more beneficial for patient prognosis compared to use after recurrence.

Methods

Objectives

The primary objective of these two trials was to observe the safety of multiple Ad-TD-nsIL12 intratumoral injections to pediatric patients with primary and progressive DIPG. The secondary objectives include 12-month OS (OS12), tumor response, immune response induced by Ad-TD-nsIL12, changes in quality of life over time, and collection of tumor and blood samples for molecular and immunological studies.

Patients

Patients were children aged 1–18 years, all of whom were diagnosed with DIPG through radiological and pathological methods. At enrollment, patients were scored for neurological function using different scoring methods according to age. The Karnofsky performance-status score (KPS score) was used for subjects aged 16 and older, while the LPS score was used for those under 16 years old. These two scores were also used for the patient's later status assessment. In addition, patients were required to have sufficient liver and kidney function, good immune function, and have not received other immunotherapies. Other detailed inclusion and exclusion criteria can be found in Tables S1 and S2.

After screening, patients were divided into two groups based on their medical history: Group A (the primary group, patients have not received any treatment) and Group B (the progressive group, patients have received radiation therapy and then experienced tumor progression). Before any treatment, patients (over 16) and their families gave informed consent.

Ethics

The study was approved by the Ethics Committee of Sanbo Brain Hospital, and registered on clinical trials website on February 8, 2023 (https://clinicaltrials.gov/study/NCT05717712 and https://clinicaltrials.gov/study/NCT05717699). The first patient was enrolled on February 15th, 2023 and last patient was enrolled on April 26th, 2023. This study adhered to the following ethical guidelines: the World Medical Association Declaration of Helsinki (https://www.wma.net/what-we-do/medical-ethics/declaration-of-helsinki/), the International Council for Harmonisation Good Clinical Practice guidelines (ICH-GCP, https://

ichgcp.net/zh), the Measures for the Ethical Review of Life Sciences and Medical Research Involving Humans (https://www.gov.cn/zhengce/zhengceku/2023-02/28/content_5743658.htm), and the Measures for the Ethical Review of Biomedical Research Involving Humans (https://www.gov.cn/zhengce/2016-10/12/content_5713806.htm). Prior to enrolment, written consent to publish clinical information (approved by Ethics Committee of Sanbo Brain Hospital) was obtained from enrolled patients or their legal representative.

Study design and treatment

These two studies are single-center, dose escalation trials. Compared to single stereotactic OV injection, multiple injections are challenging in DIPG patients. Performing multiple stereotactic punctures in the brainstem carries significant risks. Therefore, we have adopted the method of pre-implanting an Ommaya reservoir for multiple bedside OV injections. For biopsy and the insertion of the Ommaya reservoir (Sophysa RE-1201, France), a cranial MRI taken within 15 days before patient enrollment acted as the baseline scan. To ensure surgical precision, all procedures were conducted under the guidance of a REME robotic navigation system (RM-200). Postoperative head CT scans were performed to confirm the accuracy of reservoir placement. After a neuropathology expert confirmed the diagnosis of DIPG, two Ad-TD-nsIL12 injections were administered with an interval of three days. Subsequent Ad-TD-nsIL12 injections were performed every 3 weeks. The injection doses used were escalated through 3×10^{9}vp (D1), 1×10^{10}vp (D2), and 3×10^{10}vp (D3). If two or three patients developed SAE according to National Cancer Institute - Common Terminology Criteria for Adverse Events (NCI-CTCAE, version 5.0) at D1, the dose was then reduced to 1×10^{9}vp (D0).

The OV injections were administered at the bedside via a micropump into the Ommaya reservoir for approximately 1.5 h to minimize fluid reflux. The space of the Ommaya reservoir, and its volume is approximately 0.4–0.5 ml. To ensure that the predetermined drug dose accurately reaches the tumor area, we aspirate any residual liquid from the reservoir before each injection and administer an additional 0.4–0.5 mL during each injection to compensate for potential dosage loss. Therefore, the total injection volume for each administration is 1.4–1.5 ml. Group A patients underwent radiation therapy between 2 and 6 weeks post-virus treatment. Other treatments such as chemotherapy and targeted therapy were not prohibited by the trial design and were administered as determined by the physician.

Follow-ups

During the patient enrollment period, the main assessments were as follows: physical examination, neurological examination and functional status assessment (LPS or KPS scores), clinical laboratory tests, detection of adenovirus DNA and anti-adenovirus antibodies in serum, MRI scans (with or without gadolinium) and recent medication. Scheduled follow-ups were conducted at 1 week, 4 weeks, 8 weeks, and 12 weeks, respectively, after the first Ad-TD-nsIL12 injection. After 3 months, follow-up visits were performed by phone and video. Blood test results were either sent by email or delivered in person according to patient preference. Remote follow-ups were conducted approximately every 6 months. The follow-ups included: survival conditions, functional status evaluation, and documentation of AEs and concomitant medications. If any MRI scans were performed, images were collected and analyzed.

Safety evaluation

During the follow-up, AEs were graded according to NCI-CTCAE v5.0. AEs that were grade 3 or above and reached a virus treatment relevance of level 4 (Supplementary materials) or above were defined as virus-related SAEs. The same AEs in the same patient were only recorded once by the most severe case. In this study, multiple Ad-TD-nsIL12

injections were performed through the Ommaya reservoir, therefore, the assessment of viral safety ended two months after the patient's last viral treatment. Surgery, radiation therapy, and viral infections can all potentially cause edema in brainstem areas endangering patients' lives, so necessary glucocorticoids and VEGF inhibitor (such as Bevacizumab) were allowed by the protocol. Researchers fully considered medication conditions when evaluating tumor responses and additional MRI sequences were performed if necessary.

Assessment of efficacy
Cranial MRI was performed during screening and scheduled follow-ups to assess tumor response. Subsequent radiological follow-ups were carried out based on the patient's condition. Not all cases of DIPG show enhanced areas in MRI after the application of gadolinium. Therefore, in the study, T2 sequence, fluid attenuated inversion recovery (FLAIR) sequence, and T1 enhanced sequence were all analyzed and interpreted by two neurosurgical imaging experts. The RAPNO was used to assess the tumor response[29]: complete response (CR), no visible lesions for more than 8 weeks and no new lesions; PR, more than 25% reduction in lesions, and maintained for 8 weeks; PD, more than 25% increase in the smallest lesion size after baseline; SD: does not meet the criteria of CR, PR, and PD.

Flow cytometry to determine lymphocyte counts
200 μL of whole blood was incubated with 1 mL ACK lysis buffer for 3 min, then centrifuged at 4500 rpm/min for 3 min, and the supernatant discarded. This step was repeated. Cells were washed, centrifuged, resuspended in 50 μL PBS, and incubated with 2 μL FC block for 5 min. Cells were then incubated with 0.5 μL of primary antibodies (CD3-PE, 12-0038-42, ebioscience; CD8-APC, 17-0086-42, ebioscience) at 4 °C for 15 min. After washing, cells were resuspended in 200 μL PBS. Flow cytometry (Attune NxT) and FlowJo (10.4) were used for cell sorting and data analysis, with lymphocyte counts calculated from white blood cell counts and lymphocyte percentages.

Immunohistochemistry staining
IHC staining was used to assess immune response of tumor samples from biopsies. The samples were embedded in paraffin, followed by deparaffinization, antigen retrieval, and incubation with primary antibodies. The antibodies included anti-hexon of Adv (AB1056; Merck, 1:1000), anti-E1A of Adv (sc-25; Santa Cruz Biotech; 1:200), anti-CD3 (LN10; Vector Laboratories, Burlingame, CA, 1:300), anti-CD4 (VP-C320; Vector Laboratories, 1:20), anti-CD8 (VP-C320; Vector Laboratories, 1:20), anti-CD68 (MCA1957; BioRad, 1:250), anti-CD163 (ab182422; Abcam, 1:500), anti-CD86 (ab182422; Abcam, 1:500) and anti-hIL12 (EP5737; Abcam, 1:800). After incubation with biotin-labeled secondary antibodies, sections were treated with the streptavidin-peroxidase complex (Dako), followed by color development and counterstaining with hematoxylin. Finally, the slides were mounted and viewed under light microscopy (40x, Zeiss Axio Imager M2). The quantification of IHC images was conducted under 40x magnification, with six random high power fields.

Adenovirus DNA copy determination
DNA was extracted from samples using the DNeasy Blood & Tissue Kit (Qiagen, Cat: 04053228006084) according to the manufacturer's instructions. Briefly, samples were placed in 1.5 mL microcentrifuge tubes, and an appropriate volume of lysis buffer and Proteinase K was added to lyse the cells. After incubation, the lysate was transferred to a DNA binding column, where DNA was bound, washed, and eluted. The extracted DNA was then quantified using a TaqMan™ Gene Expression Master Mix (Thermo, Cat: 4369016) in a real-time quantitative PCR (qPCR) assay. The PCR reaction was conducted with the following primers: forward 5'-CCCATTGAGGTCATGGTGGAT and reverse 5'-TCAGCTGCAAGTTCTTGGGTG, using the probe FAM-

TTCACAAGCTCAAGTATGA-MGB. The qPCR data obtained were used to calculate the viral copy number in the samples.

Determination of IL-12 and other cytokines levels in plasma and cerebrospinal fluid
IL-12 levels in CSF and blood samples were measured using an ELISA kit (Invitrogen 88-7126-88) according to the manufacturer's instructions.

Other cytokine assessment was conducted by Laizee Biotech using the Luminex cytokine assay. The procedure adhered to the manufacturer's recommended protocol (Kit: EPX340-12167-901). Data acquisition was performed on the Luminex 200 instrument, and cytokine concentrations were calculated based on a five-parameter nonlinear regression standard curve.

Adenovirus antibody titer determination
Virus concentration was adjusted to 2×10^7 IU/ml. The positive control neutralizing antibody BCT004 (BioTTT001) at 3701 ng/mL was diluted in gradients of 5, 10, 500, 5000, 10000, and 50000 using 20% inactivated FBS DMEM. Test serum was pre-diluted 10-fold, with a possible further 5-fold dilution. For the neutralization assay, 50 μl of diluted antibodies and 50 μl of virus were incubated at 37 °C with 5% CO_2 for 2 h. A549 cells were centrifuged, resuspended in 10% inactivated FBS DMEM at 2×10^5 cells/ml, and added to a 96-well plate with 50 μl of the neutralized mixture. Negative controls used 10% inactivated FBS DMEM; positive controls used 50 μl of virus in 10% inactivated FBS DMEM. After 24 h of incubation at 37 °C with 5% CO_2, cells were lysed with Glo lysis buffer and Bright-Glo luciferase added. Luminescence was measured, and a standard curve from positive controls was used to calculate neutralizing antibody levels in the test serum.

Statistical analysis
AEs were summarized by population and dose group and tabulated by severity and relationship with Ad-TD-nsIL12. The data are presented using different methods based on their types: percentages (for categorical variables), median (minimum-maximum range, for non-normally distributed continuous variables), and mean ± standard deviation (for normally distributed continuous variables). OS was analyzed using Kaplan–Meier curves. OS was defined as the time from first virus injection or onset to death. Comparison of continuous variables between groups utilized repeated measures ANOVA. Data that do not follow a normal distribution were compared between groups using the Wilcoxon signed-rank test, with a significance level set at $p < 0.05$. Statistical analysis was performed using R language version 4.1.2.

Reporting summary
Further information on research design is available in the Nature Portfolio Reporting Summary linked to this article.

Data availability
Due to patient privacy concerns, certain data can be shared after review by the Ethics Committee of Sanbo Brain Hospital and by contacting the corresponding author. We welcome inquiries from interested non-profit organizations. An evaluation will be conducted, and a response will be provided within two weeks of receiving the request. If approved, the duration for which the data can be used will be defined, typically within one year. The study protocol is available in the Supplementary Information file. The remaining data are available within the Article, Supplementary Information, or Source Data file. Source data are provided with this paper.

References
1. Lieberman, N. A. P. et al. Characterization of the immune microenvironment of diffuse intrinsic pontine glioma: implications for development of immunotherapy. *Neuro-Oncol.* **21**, 83–94 (2018).

2. Caretti, V. et al. Subventricular spread of diffuse intrinsic pontine glioma. *Acta Neuropathol.* **128**, 605–607 (2014).

3. Cooney, T. et al. Contemporary survival endpoints: an International Diffuse Intrinsic Pontine Glioma Registry study. *Neuro Oncol.* **19**, 1279–1280 (2017).

4. Chan, K. M. et al. The histone H3.3K27M mutation in pediatric glioma reprograms H3K27 methylation and gene expression. *Genes Dev.* **27**, 985–990 (2013).

5. Louis, D. N. et al. The 2021 WHO classification of tumors of the central nervous system: a summary. *Neuro Oncol.* **23**, 1231–1251 (2021).

6. Lieberman, N. A. P. et al. Characterization of the immune micro-environment of diffuse intrinsic pontine glioma: implications for development of immunotherapy. *Neuro Oncol.* **21**, 83–94 (2019).

7. Harrington, K., Freeman, D. J., Kelly, B., Harper, J. & Soria, J. C. Optimizing oncolytic virotherapy in cancer treatment. *Nat. Rev. Drug Discov.* **18**, 689–706 (2019).

8. Benitez-Ribas, D. et al. Immune response generated with the administration of autologous dendritic cells pulsed with an allo-genic tumoral cell-lines lysate in patients with newly diagnosed diffuse intrinsic pontine glioma. *Front Oncol.* **8**, 127 (2018).

9. Esmaeili, M. et al. IDH1 R132H mutation generates a distinct phos-pholipid metabolite profile in glioma. *Cancer Res.* **74**, 4898–4907 (2014).

10. Gállego Pérez-Larraya, J. et al. Oncolytic DNX-2401 virus for pediatric diffuse intrinsic pontine glioma. *N. Engl. J. Med.* **386**, 2471–2481 (2022).

11. Zhang, Z. et al. A tumor-targeted replicating oncolytic adenovirus Ad-TD-nsIL12 as a promising therapeutic agent for human esopha-geal squamous cell carcinoma. *Cells* **9**, 2438 (2020).

12. Wang, P. et al. Re-designing Interleukin-12 to enhance its safety and potential as an anti-tumor immunotherapeutic agent. *Nat. Commun.* **8**, 1395 (2017).

13. Li, S. et al. Oncolytic virus Ad-TD-nsIL-12 inhibits glioma growth and reprograms the tumor immune microenvironment. *Life Sci.* **336**, 122254 (2024).

14. Ning, W. et al. Non-secreting IL12 expressing oncolytic adenovirus Ad-TD-nsIL12 in recurrent high-grade glioma: a phase I trial. *Nat. Commun.* **15**, 9299 (2024).

15. Pedretti, L. et al. Role of nutrition in pediatric patients with cancer. *Nutrients* **15**, 710 (2023).

16. Friedman, G. K. et al. Oncolytic HSV-1 G207 immunovirotherapy for pediatric high-grade gliomas. *N. Engl. J. Med.* **384**, 1613–1622 (2021).

17. Chastkofsky, M. I. et al. Mesenchymal stem cells successfully deli-ver oncolytic virotherapy to diffuse intrinsic pontine glioma. *Clin. Cancer Res.* **27**, 1766–1777 (2021).

18. Martínez-Vélez, N. et al. The oncolytic virus Delta-24-RGD elicits an antitumor effect in pediatric glioma and DIPG mouse models. *Nat. Commun.* **10**, 2235 (2019).

19. Lasek, W., Zagożdżon, R. & Jakobisiak, M. Interleukin 12: still a pro-mising candidate for tumor immunotherapy?. *Cancer Immunol. Immunother.* **63**, 419–435 (2014).

20. Chiocca, E. A. et al. Regulatable interleukin-12 gene therapy in patients with recurrent high-grade glioma: results of a phase 1 trial. *Sci. Transl. Med* **11**, eaaw5680 (2019).

21. Chiocca, E. A. et al. Combined immunotherapy with controlled interleukin-12 gene therapy and immune checkpoint blockade in recurrent glioblastoma: An open-label, multi-institutional phase I trial. *Neuro Oncol.* **24**, 951–963 (2022).

22. Malissen, B., Grégoire, C., Malissen, M. & Roncagalli, R. Integrative biology of T cell activation. *Nat. Immunol.* **15**, 790–797 (2014).

23. Paganetti, H. A review on lymphocyte radiosensitivity and its impact on radiotherapy. *Front. Oncol.* **13**, 1201500 (2023).

24. Jones, K. I. et al. Radiation combined with macrophage depletion promotes adaptive immunity and potentiates checkpoint blockade. *EMBO Mol. Med.* **10**, e9342 (2018).

25. Rückert, M., Flohr, A. S., Hecht, M. & Gaipl, U. S. Radiotherapy and the immune system: more than just immune suppression. *Stem Cells* **39**, 1155–1165 (2021).

26. Sue, M., Takeuchi, Y., Hirata, S., Takaki, A. & Otsuka, M. Impact of nutritional status on neutrophil-to-lymphocyte ratio as a predictor of efficacy and adverse events of immune check-point inhibitors. *Cancers (Basel)* **16**, 1811 (2024).

27. Liu, K. et al. Thymosin α1 reverses oncolytic adenovirus-induced M2 polarization of macrophages to improve antitumor immunity and therapeutic efficacy. *Cell Rep. Med.* **5**, 101751 (2024).

28. Liu, Y. et al. Intravenous injection of the oncolytic virus M1 awakens antitumor T cells and overcomes resistance to checkpoint block-ade. *Cell Death Dis.* **11**, 1062 (2020).

29. Erker, C. et al. Response assessment in paediatric high-grade glioma: recommendations from the Response Assessment in Pediatric Neuro-Oncology (RAPNO) working group. *Lancet Oncol.* **21**, e317–e329 (2020).

Acknowledgements

Author contributions

Concept and design: Y.W., S.W., and H.Z. Acquisition, analysis or inter-pretation of data: X.Q. and J.Y. Drafting of the manuscript: X.Q., L.C.D., H.S.P., and Y.W. Critical revision: X.Q., W.N., G.S., Y.G., D.Z., Y.Q., H.W., C.G., M.Z., Y.W., S.W., and H.Z. Statistical analysis: X.Q. Administrative, technical or material support: X.Q. and Y.W. Supervision: Y.W., S.W., and H.Z. Materials and correspondence should be addressed to Y.W., S.W., and H.Z.

Competing interests

The authors declare the following competing interests: Yaohe Wang is an inventor of the patent of Ad-TD-nsIL12 (Modified interleukin 12 and its use in manufacture of a medicament for treatment of tumors, PCT/CN2016/098527). All other authors declare no conflict of interest.

Additional information

Supplementary information The online version contains supplementary material available at https://doi.org/10.1038/s41467-025-62260-5.

Correspondence and requests for materials should be addressed to Hongwei Zhang.

Peer review information *Nature Communications* thanks Zhiyuan Liu, and the other, anonymous, reviewer(s) for their contribution to the peer review of this work. A peer review file is available.

Reprints and permissions information is available at http://www.nature.com/reprints